An Improved Denoising Algorithm for Removing Noise in Color Images

Shaveta Rani
Department of Computer Science and Applications
CT University
Ludhiana, Punjab, India
shavetabawa@pau.edu

Yogesh Chabbra
Department of Electronics and Communications
CT University
Ludhiana, Punjab, India
yogeshfzr@gmail.com

Kamal Malik
Department of Computer Science and Engineering
CT University
Ludhiana, Punjab, India
kamal.malik91@gmail.com

Abstract-Noise has a significant impact on image quality in a variety of applications, including machine vision and object recognition. Denoising is crucial for successful image processing since noisy pictures lead to erroneous findings and segmentation and enhancement mistakes. Existing methods were primarily developed for grayscale image denoising and are unable to detect all damaged pixels in an image effectively. This paper proposes a sequential ROAD-TGM-HT method to suppress impulsive noise in color image denoising. The noisy pixel location is detected using the consecutive method in the first step, and the distorted value of the damaged pixel is reconstructed in the second stage, followed by the Hough transform for the remaining undetected pixels. Peak Signal-to-Noise Ratio (PSNR) and Structural Similarity Index (SSIM) were used to analyze the qualitative and quantitative performance. ROAD-TGM-HT excels on color images with noise levels ranging from 0.10 to 0.70, as per PSNR and SSIM qualitative data.

Keywords-salt and pepper noise; ROAD-TGM; PSNR; SSIM; de-noising; impulse noise; high-density noise

I. INTRODUCTION

Digital images are frequently influenced by many types of noise caused by a variety of factors. Data transfer of images via a noisy channel, defective storage positions in hardware, and defective pixels in camera sensors during capturing images are some of the most typical causes [1-3]. Image denoising is the act of eliminating noise from an image. The main goal of image denoising is to keep image structures such as features, borders, and textures intact. It is critical to eliminate all types of noise before analyzing an image, or else there is a risk of misunderstanding [4-5]. The efficiency of an image denoising procedure is determined by the amount of noise removed from the faulty image and the recovered pixel value's similarity to the source pixel. Important information, such as edge details, will not be maintained if the image denoising approach is ineffective. During the last decades, experts have attempted to develop an effective and precise denoising technology that preserves crucial visual characteristics while reducing noise [6-8]. Various quantitative measures, such as the Peak Signal-to-Noise Ratio (PSNR), Mean Square Error (MSE), and Structural Similarity Index (SSIM), can be used to analyze the efficacy of a denoising algorithm [9-11]. Although other forms of noise alter visuals, impulse noise has the most impact. As a result, researchers concentrated on removing impulsive noise while preserving crucial information in the image [12]. In the field of image processing, the term "Salt and Pepper Noise" (SPN) is used to describe impulsive noise [13-14]. SPN occurs mostly during capture and transmission procedures. In this type of noise, certain pixels in a digital image have a maximum or minimum value. Image quality falls dramatically due to SPN.

Image denoising techniques are important to remove noise from an image. However, these approaches are often intended for grayscale images. To make these approaches functional on color images, an iterative process that can stream the components (Red, Green, and Blue) of a color image must be developed. Therefore, by dividing a color image into three components, a grayscale algorithm may be designed to work with them. Many different ways to eliminate the SPN noise from images have been presented but they don't work efficiently on color images. Considering the grayscale image, which has a single matrix with pixel intensity values ranging between 0-255, if a color image is split down into its three fundamental color components, each may be processed independently and then they can be merged to generate a colored image. Existing algorithms designed primarily for grayscale picture de-noising are unable to efficiently detect all damaged pixels in the image.

This paper proposes a composite ROAD-TGM-HT approach to remove noise from color images effectively. The

Corresponding author: Shaveta Rani

novelty of this method is that Rank-Ordered Absolute Differences with Trimmed Global Mean Filter (ROAD-TGM) has never been employed with Hough transform before. The MF [15-38], NAFSMF, DBUTMF, and ROAD-TGM were also used and their performance was compared. The performance of these approaches was evaluated using a dataset of color images with varying amounts of noise, varying from 10% to 70%.

II. LITERATURE REVIEW

A spatial filtering approach is typically employed to eliminate noise from damaged images. For denoising the image, spatial domain filters perform neighboring operations on the input image data. The numerous kinds of spatial domain filtering techniques [16-17] are Median Filter (MF) [18-36], Progressive Switching Median Filter (PSMF) [19], Center-Weighted Median Filter (CWMF) [20], Decision-Based Median Filter (DBMF) [21], Adaptive Median Filter (AMF) [22], Decision-Based Algorithm (DBA) [23], Noise Adaptive Fuzzy Switching Median Filter (NAFSMF) [24], Adaptive Weighted Mean Filter (AWMF) [25], Different Applied Median Filter (DAMF) [26], Decision Based Unsymmetric Trimmed Variant Filter (DBUTVF) [39], Modified Decision Based Unsymmetrical Trimmed Median Filter (MDBUTMF) [27], and Rank-Ordered Absolute Differences with Trimmed Global Mean Filter (ROAD-TGM) [28-29]. The Median Filter [38] performs noise filtering by replacing the median of the neighboring pixels with the value of the contaminated pixels. MF's main shortcoming is that it is only effective at very low noise levels, ranging between 10-40% noise density [30]. MF [37] typically requires a bigger window size at high noise levels and may not retain critical image information. PSMF [19] is a better version of the median filter. An impulse detector is first used to create a series of binary flag images. The position of noise is predicted by the binary flag image. An iterative approach is used to reduce image noise. The performance of this filter is low on random-valued noise, but it performs admirably for fixed-valued noise [31]. CWMF assigns a higher weight to the center values of each window, allowing key information to be preserved while noise is removed from the images [31-32]. CWMF outperforms simple MF and keeps its performance throughout a wide range of noise densities. Its execution depends on the median weight [33]. DBMF detects the existence of impulse noise among the pixels and processes the damaged image [34]. A pixel is deemed uncorrupted if its value is between 1 and 254. If the value does not fall within this range, the pixel is considered corrupted, and its value is set to the median of the neighboring pixels in the provided window. The biggest drawback of DBMF is the possibility of streaking, which happens when the image is damaged by high-density noise. In this scenario, the noisy pixel is changed by a similarly disruptive neighboring pixel value. As a result, this approach is unable to retrieve edge details adequately in large noise densities.

AMF [22] was created to address the flows of MF. Its goal is to use a dynamic adaptable window, by gradually expanding its size until the adaptive requirements are fulfilled. The window size must be sufficient to tolerate high-density noise. As a result of this, the filter's reliability and response time are

both harmed. DBA was proposed in [23] as a speedy selective median filter to reduce noise at higher densities. The median of the uncorrupted pixels was used to restore the corrupted pixels in a 3×3 selective window. DBA substitutes corrupted pixels with the earlier processed uncorrupted pixel when no uncorrupted pixel is detected in the filter window. However, DBA has the disadvantage of generating stripes in the restored images. MDBUTMF [27] was introduced as a further refinement of the previous approaches by employing the mean of the 3×3 filter to substitute corrupted pixels when no uncorrupted pixels can be detected. Although MDBUTMF eliminates the striped effect, it does not demonstrate a substantial increase in image restoration at higher noise levels. AWMF [25] employs an approach to determine if a pixel is uncorrupted by comparing its intensity with the range between the filtering window with minimum and maximum noise intensities. The mean of the uncorrupted pixels in the filtering window is used as a substitute for the identified corrupted pixels. If no uncorrupted pixels are detected in the filtering window, the filtering window is enlarged in size. AWMF takes longer to process due to its adaptive nature. NAFSMF [24] uses a dynamic adaptive window. A fuzzy decision-making approach determines a new value for NAFSMF. NAFSMF is also effective in suppressing high-density noise. DAMF [26] is capable of handling all impulse noise densities. The ROAD-TGM method employs a trimmed global mean filter with rank-ordered absolute differences [35] and is processed in two phases. In the first stage, ROAD is used to determine noisy pixels. The noisy pixels are transformed to the median of the non-noisy pixels inside a chosen window in the second stage. When the chosen window only includes corrupted pixels, the TGM filter is employed. This method employs a fixed-size window in both the filtering and detection stages. When recovering images impacted by random-valued impulse noise, its denoising performance outperforms other known methods. When images are distorted by high amounts of impulse noise, the ROAD-TGM algorithm delivers effective noise filtering.

These methods work in two stages: (i) detecting noisy pixels and (ii) restoring them. However, it has been observed that certainly damaged pixels aren't picked during the identification stage and remain corrupted. This study employed the Hough transform to find the remaining pixels. The proposed method uses ROAD and TGM to identify damaged pixels and the Hough transform which forms lines on a denoised image and fills those pixels by calculating the mean of the uncorrupted pixels.

III. PROPOSED METHOD

A 5×5 detection window (W) centered on $I(i, j)$ was implemented on the damaged image. In [40], a 3×3 window with $m = 4$ is recommended for less than 25% noise density, otherwise, a 5×5 window with $m = 12$ is recommended. Increasing the filter size causes blurring. The following equation is used to calculate the absolute difference (D) of all pixel values with the center pixel:

$$D = |W(i + k, j + l) - W(i,j)|, -LD \leq k, l \leq LD \quad (1)$$

The sum of the twelve lowest absolute differences is computed after sorting the array *D*. This produces the ROAD value for the current pixel as:

$$ROAD_m(x) = \sum_{i=1}^{m} ri(x) \quad (2)$$

The current pixel's ROAD value is compared to a specified threshold value. The current pixel is considered damaged or uncontaminated based on the threshold value. Threshold values affect the performance of noise detection. As the threshold value raises, an increasing number of noise-free pixels are left unfiltered. The filtering is conducted solely on noisy pixels at a specific threshold value, which is referred to as ideal. The noise-removing effectiveness of filtering is reduced when the threshold is increased further because the filtering is not applied to certain noisy pixels. When set to the ideal threshold setting, the filter successfully maintains tiny lines and other fine details. For the best results, the threshold value for all images was set at 40, but this value can change depending on the dataset. The foregoing processes are repeated for the complete image, resulting in a binary image (*I*) of size *M×N*.

$$A = \left\langle {1 \atop 0} \right\rangle {{\text{For } ROAD(i,j) < T1} \atop {\text{For } ROAD(i,j) > T1}} \quad (3)$$

The noiseless pixels in the specified window are used to replace the deteriorated pixels. A trimmed global mean filter is used if the chosen window contains only noise-impacted pixels. The TGM is then computed once the noise has been removed. The pixels from the window and the mean of the uncorrupted pixels are acquired to replace the value of a noisy pixel. The proposed method used ROAD and TGM to identify damaged pixels at first and then uses the Hough Transform to fill the remaining pixels not captured by ROAD-TGM. The Hough transform creates lines between the corrupted pixels on a denoised image, calculates the mean of the denoised image after creating lines, and fills those pixels with the mean of the uncorrupted pixels. Figure 2 represents the flow diagram of the restoration process. Various images from the USC dataset [41] of standard color images were used for simulation, as shown in Figure 1. All images were 512×512 in tiff format, with intentionally added noise ranging from 0.10 to 0.70.
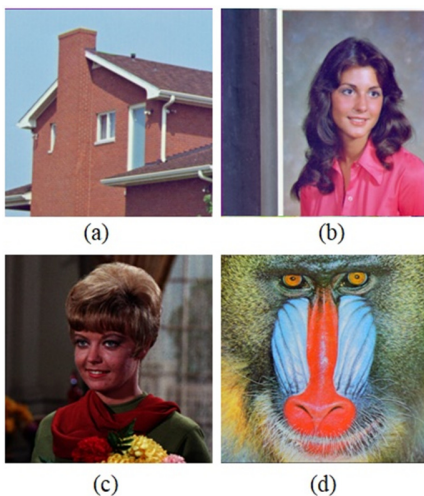

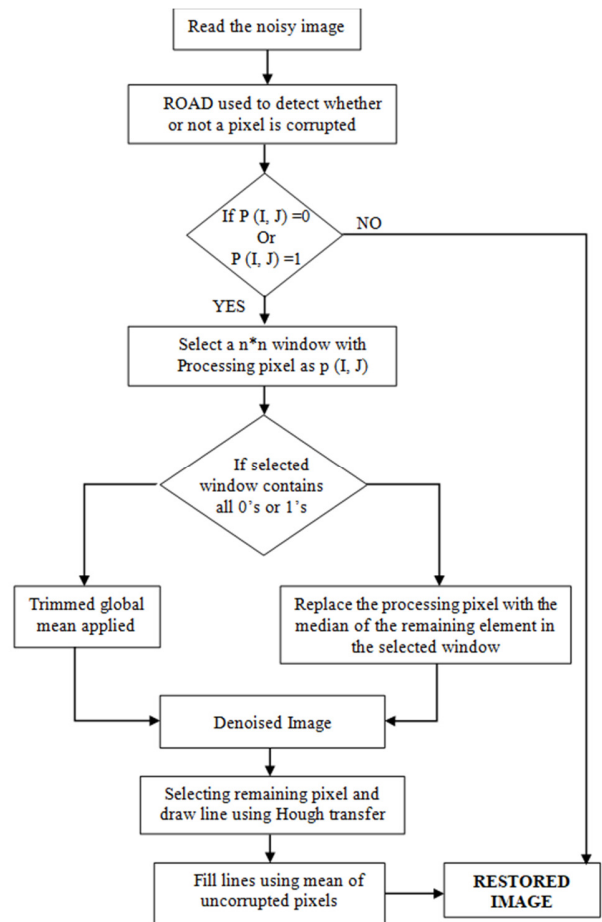Fig. 1.   Original images: (a) Hut, (b) Female, (c) Zelda, (d) Baboon.

Fig. 2.   Flowchart representing the proposed method for restoration.

IV. EXPERIMENTAL RESULTS AND DISCUSSION

The tests were performed using MATLAB R2007b. Image Quality Assessment Metrics, such as MSE and PSNR, were used to evaluate the performance of the image denoising algorithms by measuring the quality of the processed image in contrast to the original. PSNR, which is expressed in decibels (dB) and is calculated as the ratio of a signal's maximum achievable power to the disruptive noise power. Higher PSNR indicates a greater performance, and the lower the PSNR value, the worse the performance of a denoising method. Equations (4) and (5) were used to calculate PSNR and MSE:

$$PSNR\ (dB) = 10 * log10\ ((255 \times 255)/MSE) \quad (4)$$

$$MSE = \frac{1}{P \times Q} \sum_{i=1}^{p} \sum_{j=1}^{q} (I_d(i,j) - I_o(i,j))^2 \quad (5)$$

where $I_O(i, j)$ with size *P×Q*, $I_d(i, j)$ represents the denoised image created by the denoising algorithm.

SSIM measures the loss of image quality due to activities such as data transfer and compression. SSIM [45] is used to assess the perceived quality of digital movies and images. It is a complete reference measure that is calculated using two images: the reference image is the original and the resultant image is the second. SSIM calculates the brightness (*b*), contrast (*c*), and structure (*s*) of *x* and *y* images, as:

$$SSIM(x; y) = [b(x; y)]\alpha[c(x; y)]\beta[s(x; y)]\gamma \quad (6)$$

This section compares the proposed method to current algorithms for assessment. As previously stated, multiple noise densities were progressively applied to each image, ranging from 20% to 70% noise level, resulting in sequences of the increasingly distorted image with impulsive noise. The PSNR graph is shown in Figure 3 for the Baboon, Female, Hut, and Zelda images. Figures 4-7 illustrate the denoised images generated using the various methods.
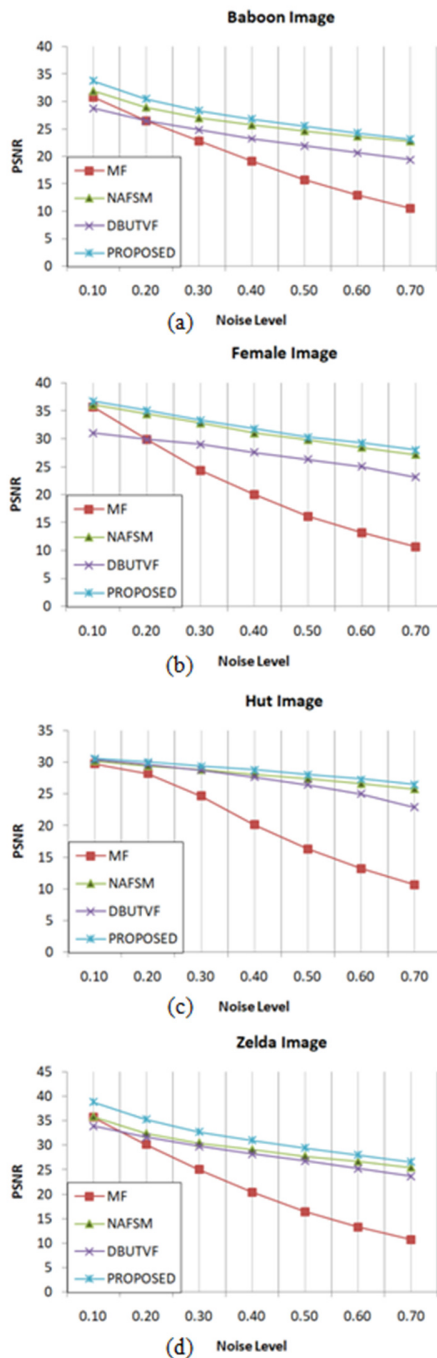

Fig. 3.   PSNR Graphs: (a) Baboon, (b) Female, (c) Hut, and (d) Zelda.

Fig. 4.   (aa –af) Hut images corrupted by 20-70%, restored images using: (ba–bf) MF, (ca–cf) NAFSM, (da–df) DBUTVF, (ea–ef) proposed method.
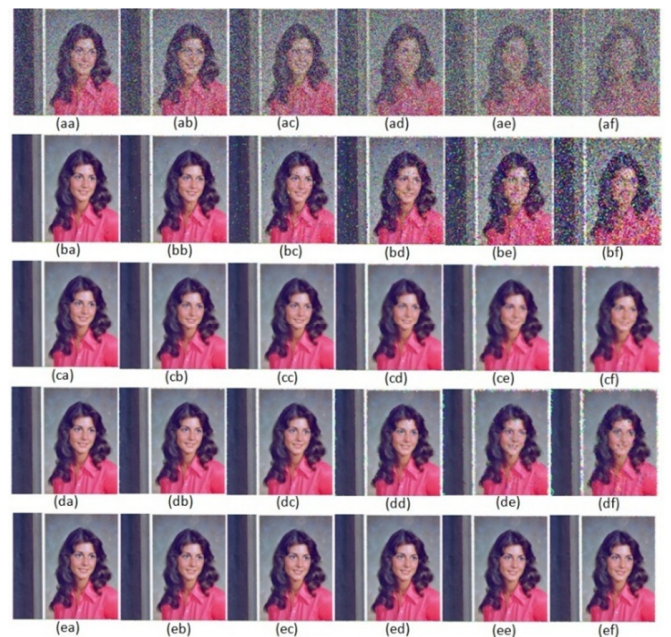

Fig. 5.   (aa–af) Female images corrupted 20-70%, restored images using: (ba–bf) MF, (ca–cf) NAFSM, (da–df) DBUTVF, (ea–ef) proposed method.

Table I compares the proposed method with the state-of-the-art denoising algorithms on images with noise levels ranging in 10-70%. Different simulation tests were carried out on the test images, which were corrupted with impulse noise. All methods were evaluated using PSNR and SSIM values. The proposed ROAD-TGM-HT method was compared with MF, NAFSM, and DBUTVF to remove impulsive noise from the image, and the results showed that it outperformed them, consistently providing higher PSNR and SSIM values.
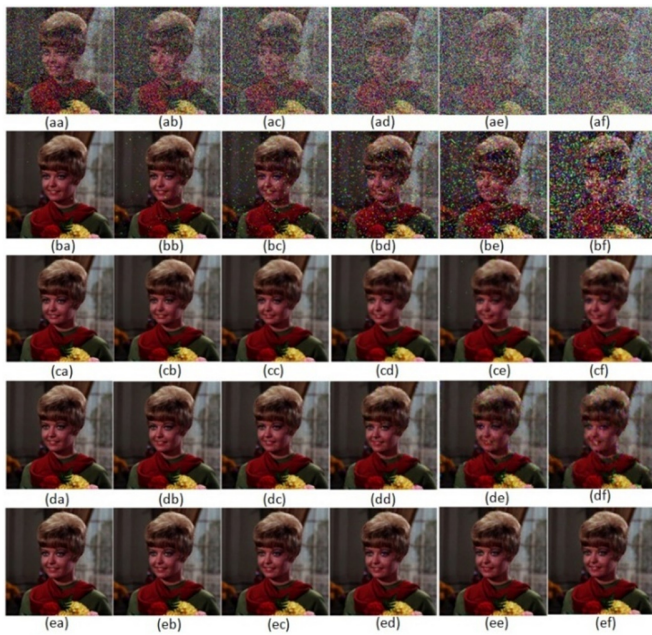
Fig. 6.   (aa–af) Zelda images corrupted by 20-70%, restored images using: (ba–bf) MF, (ca–cf) NAFSM, (da–df) DBUTVF, (ea–ef) proposed method.
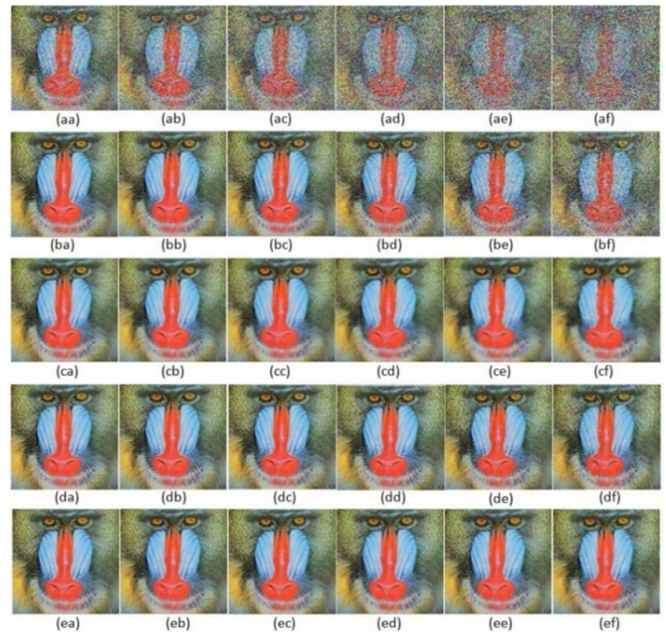

Fig. 7.   (aa–af) Baboon image corrupted 20% -70%, restored images using: (ba – bf) MF, (ca–cf) NAFSM, (da–df) DBUTVF, (ea–ef) proposed method.

TABLE I.   COMPARISON OF DIFFERENT TYPES OF DENOISING FILTERS WITH PSNR AND SSIM VALUES.

Image	Noise Density		0.10	0.20	0.30	0.40	0.50	0.60	0.70
Hut	MF [17-18]	PSNR	29.81	28.29	24.72	20.18	16.36	13.23	10.67
		SSIM	0.9926	0.9694	0.8988	0.7390	0.5349	0.3314	0.1925
	NAFSM [24]	PSNR	30.23	29.48	28.85	28.16	27.43	26.65	25.81
		SSIM	0.9843	0.9772	0.9700	0.9605	0.9500	0.9383	0.9221
	DBUTVF [39]	PSNR	30.48	29.67	28.79	27.68	26.51	25.06	22.92
		SSIM	0.9857	0.9788	0.9698	0.9554	0.9359	0.9088	0.8661
	PROPOSED	**PSNR**	**30.63**	**30.11**	**29.45**	**28.82**	**28.04**	**27.34**	**26.49**
		SSIM	**0.9870**	**0.9825**	**0.9763**	**0.9687**	**0.9600**	**0.9494**	**0.9350**
Baboon	MF [17-18]	PSNR	30.80	26.53	22.86	19.15	15.73	12.89	10.50
		SSIM	0.9761	0.9375	0.8636	0.7326	0.5607	0.3892	0.2499
	NAFSM [24]	PSNR	31.96	28.98	27.00	25.73	24.65	23.66	22.74
		SSIM	0.9758	0.9503	0.9223	0.8944	0.8594	0.8243	0.7826
	DBUTV [39]	PSNR	28.77	26.48	24.80	23.26	21.95	20.70	19.40
		SSIM	0.9706	0.9436	0.9112	0.8711	0.8241	0.7658	0.6964
	PROPOSED	**PSNR**	**33.80**	**30.52**	**28.37**	**26.83**	**25.53**	**24.32**	**23.13**
		SSIM	**0.9830**	**0.9637**	**0.9416**	**0.9172**	**0.8872**	**0.8528**	**0.8180**
Zelda	MF [17-18]	PSNR	38.59	31.06	25.32	20.02	15.93	12.60	10.08
		SSIM	0.9872	0.9466	0.8155	0.5824	0.3471	0.1943	0.1067
	NAFSM [24]	PSNR	37.64	34.66	32.60	31.07	30.04	29.12	28.01
		SSIM	0.9874	0.9750	0.9614	0.9487	0.9325	0.9173	0.8915
	DBUTVF [39]	PSNR	39.11	35.44	33.51	31.17	29.46	27.27	25.52
		SSIM	0.9880	0.9760	0.9611	0.9390	0.9155	0.8836	0.8353
	PROPOSED	**PSNR**	**40.72**	**37.63**	**35.24**	**33.41**	**32.08**	**30.69**	**29.19**
		SSIM	**0.9917**	**0.9828**	**0.9716**	**0.9591**	**0.9446**	**0.9271**	**0.9052**
Female	MF [17-18]	PSNR	35.73	29.94	24.36	20.00	16.10	13.15	10.64
		SSIM	0.9921	0.9596	0.8652	0.6694	0.4480	0.2739	0.1637
	NAFSM [24]	PSNR	36.13	34.51	32.87	31.06	29.88	28.50	27.23
		SSIM	0.9934	0.9882	0.9800	0.9724	0.9632	0.9518	0.9328
	DBUTVF [39]	PSNR	31.05	29.90	29.01	27.57	26.35	25.03	23.17
		SSIM	0.9813	0.9788	0.9698	0.9554	0.9359	0.9088	0.8661
	PROPOSED	**PSNR**	**36.75**	**35.16**	**33.28**	**31.84**	**30.31**	**29.28**	**28.02**
		SSIM	**0.9946**	**0.9903**	**0.9844**	**0.9770**	**0.9671**	**0.9562**	**0.9421**

V. Conclusion

This paper presented an improved sequential ROAD-TGM-HT filter to reduce high-density noise from color images while preserving precise image features. To test the efficiency of the proposed method, varying degrees of noise from 10% to 70% were applied to a large dataset of color images, and then their PSNR and SSIM values were measured after denoising. The proposed de-noising method outperformed other known algorithms in terms of PSNR and SSIM. The suggested approach can be improved by improving the initial value estimation stage.

References

[1] A. Singh, G. Sethi, and G. S. Kalra, "Spatially Adaptive Image Denoising via Enhanced Noise Detection Method for Grayscale and Color Images," *IEEE Access*, vol. 8, pp. 112985–113002, 2020, https://doi.org/10.1109/ACCESS.2020.3003874.

[2] D. Aspandi, O. Martinez, F. Sukno, and X. Binefa, "Composite recurrent network with internal denoising for facial alignment in still and video images in the wild," *Image and Vision Computing*, vol. 111, Jul. 2021, Art. no. 104189, https://doi.org/10.1016/j.imavis.2021.104189.

[3] D. G. Kim, M. Hussain, M. Adnan, M. A. Farooq, Z. H. Shamsi, and A. Mushtaq, "Mixed Noise Removal Using Adaptive Median Based Non-Local Rank Minimization," *IEEE Access*, vol. 9, pp. 6438–6452, 2021, https://doi.org/10.1109/ACCESS.2020.3048181.

[4] A. Mukherjee, S. Sarkar, and S. K. Saha, "Segmentation of natural images based on super pixel and graph merging," *IET Computer Vision*, vol. 15, no. 1, pp. 1–11, 2021, https://doi.org/10.1049/cvi2.12008.

[5] A. Jindal, N. Aggarwal, and S. Gupta, "An Obstacle Detection Method for Visually Impaired Persons by Ground Plane Removal Using Speeded-Up Robust Features and Gray Level Co-Occurrence Matrix," *Pattern Recognition and Image Analysis*, vol. 28, no. 2, pp. 288–300, Apr. 2018, https://doi.org/10.1134/S1054661818020086.

[6] I. Aizenberg, C. Butakoff, and D. Paliy, "Impulsive noise removal using threshold Boolean filtering based on the impulse detecting functions," *IEEE Signal Processing Letters*, vol. 12, no. 1, pp. 63–66, Jan. 2005, https://doi.org/10.1109/LSP.2004.838198.

[7] F. Jing, H. Shaohai, and M. Xiaole, "SAR image de-noising via grouping-based PCA and guided filter," *Journal of Systems Engineering and Electronics*, vol. 32, no. 1, pp. 81–91, Oct. 2021, https://doi.org/10.23919/JSEE.2021.000009.

[8] L. Zhang, J. Liu, F. Shang, G. Li, J. Zhao, and Y. Zhang, "Robust segmentation method for noisy images based on an unsupervised denosing filter," *Tsinghua Science and Technology*, vol. 26, no. 5, pp. 736–748, Jul. 2021, https://doi.org/10.26599/TST.2021.9010021.

[9] S. Kaisar, S. Rijwan, J. A. Mahmud, and M. M. Rahman, "Salt and Pepper Noise Detection and removal by Tolerance based Selective Arithmetic Mean Filtering Technique for image restoration," *International Journal of Computer Science and Network Security*, vol. 8, no. 6, pp. 271–278, Jun. 2008.

[10] X. Fei, L. Xiao, Y. Sun, and Z. Wei, "Perceptual image quality assessment based on structural similarity and visual masking," *Signal Processing: Image Communication*, vol. 27, no. 7, pp. 772–783, Aug. 2012, https://doi.org/10.1016/j.image.2012.04.005.

[11] G. M. Daiyan and M. A. Mottalib, "Removal of high density salt amp; pepper noise through a modified decision based median filter," in *2012 International Conference on Informatics, Electronics Vision (ICIEV)*, Feb. 2012, pp. 565–570, https://doi.org/10.1109/ICIEV.2012.6317448.

[12] P. S. Windyga, "Fast impulsive noise removal," *IEEE Transactions on Image Processing*, vol. 10, no. 1, pp. 173–179, Jan. 2001, https://doi.org/10.1109/83.892455.

[13] T. Chen and H. R. Wu, "Application of partition-based median type filters for suppressing noise in images," *IEEE Transactions on Image Processing*, vol. 10, no. 6, pp. 829–836, Jun. 2001, https://doi.org/10.1109/83.923279.

[14] A. Noor, Y. Zhao, R. Khan, L. Wu, and F. Y. O. Abdalla, "Median filters combined with denoising convolutional neural network for Gaussian and impulse noises," *Multimedia Tools and Applications*, vol. 79, no. 25, pp. 18553–18568, Jul. 2020, https://doi.org/10.1007/s11042-020-08657-4.

[15] H. Zeng, Y. Z. Liu, Y. M. Fan, and X. Tang, "An Improved Algorithm for Impulse Noise by Median Filter," *AASRI Procedia*, vol. 1, pp. 68–73, Jan. 2012, https://doi.org/10.1016/j.aasri.2012.06.014.

[16] W. Fan, H. Yu, T. Chen, and S. Ji, "OCT Image Restoration Using Non-Local Deep Image Prior," *Electronics*, vol. 9, no. 5, May 2020, Art. no. 784, https://doi.org/10.3390/electronics9050784.

[17] T. Chen, K. K. Ma, and L. H. Chen, "Tri-state median filter for image denoising," *IEEE Transactions on Image Processing*, vol. 8, no. 12, pp. 1834–1838, Sep. 1999, https://doi.org/10.1109/83.806630.

[18] C. C. Chang, J. Y. Hsiao, and C. P. Hsieh, "An Adaptive Median Filter for Image Denoising," in *Proceedings of the 2008 Second International Symposium on Intelligent Information Technology Application - Volume 02*, Sep. 2008, pp. 346–350, https://doi.org/10.1109/IITA.2008.259.

[19] S. T. Boo, H. Ibrahim, and K. K. V. Toh, "An Improved Progressive Switching Median Filter," in *2009 International Conference on Future Computer and Communication*, Kuala Lumpar, Malaysia, Apr. 2009, pp. 136–139, https://doi.org/10.1109/ICFCC.2009.87.

[20] S. J. Ko and Y. H. Lee, "Center weighted median filters and their applications to image enhancement," *IEEE Transactions on Circuits and Systems*, vol. 38, no. 9, pp. 984–993, Sep. 1991, https://doi.org/10.1109/31.83870.

[21] R. Kunsoth and M. Biswas, "Modified decision based median filter for impulse noise removal," in *2016 International Conference on Wireless Communications, Signal Processing and Networking (WiSPNET)*, Chennai, India, Mar. 2016, pp. 1316–1319, https://doi.org/10.1109/WiSPNET.2016.7566350.

[22] H. Hwang and R. A. Haddad, "Adaptive median filters: new algorithms and results," *IEEE Transactions on Image Processing*, vol. 4, no. 4, pp. 499–502, Apr. 1995, https://doi.org/10.1109/83.370679.

[23] K. S. Srinivasan and D. Ebenezer, "A New Fast and Efficient Decision-Based Algorithm for Removal of High-Density Impulse Noises," *IEEE Signal Processing Letters*, vol. 14, no. 3, pp. 189–192, Mar. 2007, https://doi.org/10.1109/LSP.2006.884018.

[24] K. K. V. Toh and N. A. Mat Isa, "Noise Adaptive Fuzzy Switching Median Filter for Salt-and-Pepper Noise Reduction," *IEEE Signal Processing Letters*, vol. 17, no. 3, pp. 281–284, Mar. 2010, https://doi.org/10.1109/LSP.2009.2038769.

[25] P. Zhang and F. Li, "A New Adaptive Weighted Mean Filter for Removing Salt-and-Pepper Noise," *IEEE Signal Processing Letters*, vol. 21, no. 10, pp. 1280–1283, Jul. 2014, https://doi.org/10.1109/LSP.2014.2333012.

[26] U. Erkan, L. Gökrem, and S. Enginoğlu, "Different applied median filter in salt and pepper noise," *Computers & Electrical Engineering*, vol. 70, pp. 789–798, Aug. 2018, https://doi.org/10.1016/j.compeleceng.2018.01.019.

[27] S. Esakkirajan, T. Veerakumar, A. N. Subramanyam, and C. H. PremChand, "Removal of High Density Salt and Pepper Noise Through Modified Decision Based Unsymmetric Trimmed Median Filter," *IEEE Signal Processing Letters*, vol. 18, no. 5, pp. 287–290, Feb. 2011, https://doi.org/10.1109/LSP.2011.2122333.

[28] G. S. Kalra and S. Singh, "Efficient digital image denoising for gray scale images," *Multimedia Tools and Applications*, vol. 75, no. 8, pp. 4467–4484, Apr. 2016, https://doi.org/10.1007/s11042-015-2484-x.

[29] A. Singh, G. Sethi, and G. S. Kalra, "Amalgamation of ROAD-TGM and progressive PCA using performance booster method for detail persevering image denoising," *Multimedia Tools and Applications*, vol. 81, no. 2, pp. 1719–1742, Jan. 2022, https://doi.org/10.1007/s11042-021-11426-6.

[30] U. Erkan, D. N. H. Thanh, L. M. Hieu, and S. Engínoğlu, "An Iterative Mean Filter for Image Denoising," *IEEE Access*, vol. 7, pp. 167847–167859, 2019, https://doi.org/10.1109/ACCESS.2019.2953924.

[31] S. J. Ko and Y. H. Lee, "Center weighted median filters and their applications to image enhancement," *IEEE Transactions on Circuits and*

Systems, vol. 38, no. 9, pp. 984–993, Sep. 1991, https://doi.org/10.1109/31.83870.

[32] R. H. Chan, C. Hu, and M. Nikolova, "An iterative procedure for removing random-valued impulse noise," *IEEE Signal Processing Letters*, vol. 11, no. 12, pp. 921–924, Sep. 2004, https://doi.org/10.1109/LSP.2004.838190.

[33] K. Aiswarya, V. Jayaraj, and D. Ebenezer, "A New and Efficient Algorithm for the Removal of High Density Salt and Pepper Noise in Images and Videos," in *2010 Second International Conference on Computer Modeling and Simulation*, Jan. 2010, vol. 4, pp. 409–413, https://doi.org/10.1109/ICCMS.2010.310.

[34] G. M. Daiyan and M. A. Mottalib, "Removal of high density salt amp; pepper noise through a modified decision based median filter," in *2012 International Conference on Informatics, Electronics Vision (ICIEV)*, Feb. 2012, pp. 565–570, https://doi.org/10.1109/ICIEV.2012.6317448.

[35] A. Singh, G. Sethi, and G. S. Kalra, "Amalgamation of ROAD-TGM and progressive PCA using performance booster method for detail persevering image denoising," *Multimedia Tools and Applications*, vol. 81, no. 2, pp. 1719–1742, Jan. 2022, https://doi.org/10.1007/s11042-021-11426-6.

[36] S. Banerjee, A. Bandyopadhyay, A. Mukherjee, A. Das, and R. Bag, "Random Valued Impulse Noise Removal Using Region Based Detection Approach," *Engineering, Technology & Applied Science Research*, vol. 7, no. 6, pp. 2288–2292, Dec. 2017, https://doi.org/10.48084/etasr.1609.

[37] V. Yatnalli, B. G. Shivaleelavathi, and K. L. Sudha, "Review of Inpainting Algorithms for Wireless Communication Application," *Engineering, Technology & Applied Science Research*, vol. 10, no. 3, pp. 5790–5795, Jun. 2020, https://doi.org/10.48084/etasr.3547.

[38] K. H. Hii, V. Narayanamurthy, and F. Samsuri, "ECG Noise Reduction with the Use of the Ant Lion Optimizer Algorithm," *Engineering, Technology & Applied Science Research*, vol. 9, no. 4, pp. 4525–4529, Aug. 2019, https://doi.org/10.48084/etasr.2766.

[39] K. Vasanth, V. Jawahar Senthilkumar, and V. Rajesh, "A Decision based Unsymmetrical Trimmed Variants for the Removal of High Density Salt and Pepper Noise," *International Journal of Computer Applications*, vol. 42, no. 15, pp. 38–43, Mar. 2012, https://doi.org/10.5120/5772-8166.

[40] R. Garnett, T. Huegerich, C. Chui, and W. He, "A universal noise removal algorithm with an impulse detector," *IEEE Transactions on Image Processing*, vol. 14, no. 11, pp. 1747–1754, Aug. 2005, https://doi.org/10.1109/TIP.2005.857261.

[41] USC - University of Southern California, "SIPI Image Database - Misc." https://sipi.usc.edu/database/database.php?volume=misc (accessed May 02, 2022).